GEOPHYSICAL RESEARCH LETTERS, VOL. 22, NO. 16, PAGES 2091-2094, AUGUST 15, 1995

Electron dynamics and whistler waves at quasi-perpendicular shocks

D. Krauss-Varban

Department of Electrical and Computer Engineering, University of California, San Diego, La Jolla

F. G. E. Pantellini[1] and D. Burgess

Astronomy Unit, Queen Mary and Westfield College, London

Abstract. The collisionless, supercritical, quasi-perpendicular fast shock is investigated on sub-ion scales using an implicit, two-dimensional (2-D) full particle code. For the first time, simulations are carried out with realistic characteristic frequencies and sufficiently high mass ratio between the protons and electrons. As a result, there is relatively little scattering of the electrons, i.e., they behave largely adiabatically as previously suggested based on spacecraft observations at the Earth's bow shock. The large mass ratio also allows for a realistic description of the whistler mode dispersion. Phase-standing whistlers with propagation along the shock normal appear as transients. The dominant whistlers found at late times in the simulations have upstream directed group velocity but propagate at oblique direction between the shock normal and the ambient magnetic field. Their properties match those of the ubiquitous observed upstream whistlers ("one-Hertz waves").

1. Introduction

Through a combination of spacecraft observations, theory, and simulations, much progress has been made in our understanding of collisionless shocks, such as the Earth's and other planetary bow shocks. At supercritical quasi-perpendicular shocks (angle between the upstream magnetic field $\mathbf{B_0}$ and shock normal $\mathbf{n}$ is $\theta_{Bn} \gtrsim 45°$), ion thermalization and the global shock structure are dominated by reflected ions, which are convected back into the shock [*Leroy et al.,* 1982; *Sckopke et al.,* 1983; *McKean et al.,* 1995, and references therein]. Compared to the ions, electron thermalization and associated wave processes are only understood to a much lesser extent. The microphysical description of the electrons constitutes one of the outstanding problems of shock physics. It is not known to what extent the ion and electron dynamics at the shock are coupled. This paper presents initial results of two-dimensional (2-D) implicit full particle simulations that are carried out to address this topic.

Observationally, a number of points relevant to the present study have been established: (1) The Earth's bow shock shows various features in the electron velocity distribution such as a loss-cone, temperature anisotropies, and beams before a thermalized, flat-topped distribution is reached downstream [*Feldman et al.,* 1983]. (2) Still, the observed distributions are consistent with the idea that electrons behave mostly adiabatically (i.e., conserving the magnetic moment), with only moderate scattering that may fill in otherwise inaccessible parts of the phase space [*Feldman et al.,* 1983; *Scudder et al.,* 1986]. (3) While the overall shock ramp appears to be of the order of the proton inertial length c/ω_p, the steepest part may have an exponential scale that is only a fraction of that ($\sim 0.2\ c/\omega_p$, *Scudder et al.* [1986]). (4) In addition to electrostatic turbulence, electromagnetic whistler waves are observed both upstream and in the shock transition [*Gurnett,* 1985]. In the upstream, these waves were sometimes called "one-Hertz waves" [*Hoppe and Russell,* 1983] but are now simply referred to as "upstream whistlers" [*Orlowski et al.,* 1993, 1995].

It is generally believed that in addition to the macroscopic fields, which determine the overall mapping of the distribution function, the above mentioned waves are responsible for the pitch-angle scattering (and any additional thermalization) of the electrons [*Feldman et al.,* 1983; *Krauss-Varban,* 1992; *Veltri and Zimbardo,* 1993]. However, a genuine physical explanation of the wave generation, electron dynamics, and any sub-ion scale shock structure requires analysis of the evolution of the electron distribution in the self-consistent fields. The ideal tool for such a study are particle simulations which include processes in which both electrons and ions are involved. Due to the different temporal and spatial scales of these particles, such simulations are extremely difficult to perform. Below we show that for a realistic ordering of the frequencies and to capture the correct propagation characteristics of the waves, a large mass ratio between the protons and electrons is necessary. Simply speaking, a low mass ratio implies artificially strong coupling between the protons and electrons. This affects not only the wave properties but also leads to unphysical heating of the electrons and protons. Since most previous simulations employed the conventional explicit particle codes [*Forslund et al.,* 1984; *Lembège and Dawson,* 1987; *Savoini and Lembège,* 1994], which require time steps smaller than the inverse electron plasma frequency, the goal of a realistic mass ratio could not be achieved except in short duration 1-D simulations [*Liewer et al.,* 1991]. Making use of an implicit full particle code, which does not have the above time step restriction, we present here for the first time results of realistic, large mass-ratio 2-D shock simulations.

[1]Now at DESPA, Observatoire de Paris, Meudon, France.

Paper number 95GL01782
0094-8534/95/95GL-01782$03.00

2. Simulation

The implicit, full particle simulation code is based on the so-called direct (predictor-corrector) method as described by *Hewett and Langdon* [1987], with several improvements due to *Heron and Adam* [1989]. A variant of this code has previously been used for simulations of the quasi-parallel bow shock [*Pantellini et al.*, 1992]. The particles and fields are initialized according to Rankine-Hugoniot, with an initial linear shock ramp 4 c/ω_e wide in the center of the box. Particles are continuously injected and allowed to escape at both sides (along the x-axis) to maintain upstream and downstream Maxwellian distributions. The total flux through the system is constant such that the shock remains in the center of the box, and the number of simulation particles is kept constant. The -**x** direction is aligned with the shock normal **n**. The second simulation direction is along **y** with periodic boundary conditions. The upstream magnetic field $\mathbf{B_o}$ is kept in the simulation plane, making an angle of $\theta_{Bn} = 60°$ with the shock normal. The other plasma parameters are set to reflect generic bow shock conditions: the Alfvén Mach number is $M_A = 5$, and the electron and ion upstream beta are $\beta_e = \beta_i = 0.5$.

The electron plasma to cyclotron frequency ratio is $\omega_e/\Omega_e = 100$ and the proton to electron mass ratio is set to $m_p/m_e = 400$. This separates the characteristic frequencies (ω_e, Ω_e, Ω_{LH}, Ω_p) by more than an order of magnitude each. Here, Ω_{LH} is the lower hybrid frequency and Ω_p is the proton cyclotron frequency. Also, this gives a ratio of $(c/\omega_p)/(c/\omega_e) = 20$ between the proton and electron inertial lengths. The cell sizes are $\Delta x = 0.25\ c/\omega_e$ and $\Delta y = 1.0\ c/\omega_e$, with a box size $X \times Y$ of 1600×64 cells or $20 \times 3.2\ c/\omega_p$, and an average of 20 particles per cell for each species. The simulation is run in two parts with 10,000 time steps each. The initial part has a time step $\Delta t = 0.16\ \Omega_e^{-1}$, the second part has 1/2 of this to properly resolve the electron gyromotion. The total run time is $6\ \Omega_p^{-1}$. The above parameters are carefully balanced to satisfy numerical conditions, allow a sufficiently large space-time domain, and avoid excessive numerical cooling or scattering within a feasible total CPU.

For the fast mode shock transition, and to differentiate between shock-generated phase-standing and instability-generated propagating waves, it is crucial to describe the whistler dispersion properly. Figure 1 shows the dispersion relation $\omega(k)$ normalized to ion scales and in the shock frame for several mass ratios m_p/m_e, as indicated. The propagation angle is (a) $\theta_{kB} = 30°$, i.e., wavevector **k** between $-\mathbf{B_o}$ and **n**, and (b) $\theta_{kB} = 60°$, i.e., **k** || **n**. Except for the scale there are few differences. One can conclude that a value of $m_p/m_e \sim 400$, as employed here, is necessary to capture waves that are approximately phase standing or that have an upstream directed group velocity $\partial\omega/\partial k > 0$.

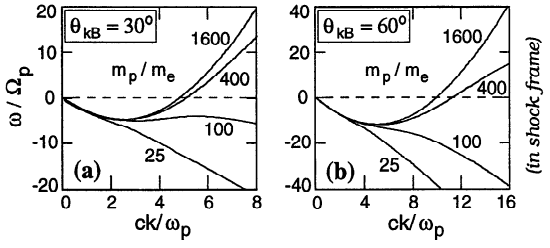

Figure 1. Dispersion relation $\omega(k)$ for whistler waves (a) propagating at an angle $\theta_{kB} = 30°$ and (b) at $\theta_{kB} = 60°$ with respect to $\mathbf{B_o}$, for mass ratios as indicated.

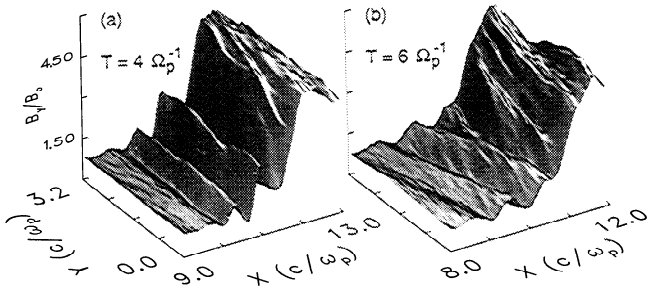

Figure 2. Compressional magnetic field component at (a) early and (b) late time in the simulation. Note the transition from phase-standing waves to oblique, upstream propagating whistlers.

3. Results and Discussion

In this letter we concentrate on the overall shock solution, whistler waves, and the general electron phase space evolution. A more detailed description of the simulation results will be given in a forthcoming publication.

For the Mach numbers common to the front of the bow shock, no phase-standing whistler wave train is found in satellite observations. Such whistlers would be expected to form in a sufficiently thin and steady shock ramp as part of the steepening/evolution of the shock, and should propagate along the shock normal [*cf. Tidman and Northrop*, 1968]. Instead, the whistlers observed in the ramp and upstream propagate at an angle to **n** and have varying phase velocities, although they are still mainly confined to the plane of $\mathbf{B_o}$ and **n** [*Orlowski and Russell*, 1991]. Typical propagation angles between **k** and $\mathbf{B_o}$ at both Earth and Venus are $20° \leq \theta_{kB} \leq 40°$ [*Fairfield*, 1974; *Orlowski and Russell*, 1991], with a strong preference for $\sim 40°$ [*Fairfield*, 1974; *Hoppe et al.*, 1982]. The decreasing amplitude away from the shock led Fairfield to suggest that the waves are generated in the ramp; a more thorough analysis by *Orlowski et al.* [1995] has recently confirmed this and has shown independent evidence that the waves are not generated in situ in the upstream. A lower frequency cut-off has been found to correspond to a wavelength of $\sim 1\ c/\omega_p$, with the conjecture that it coincides with the shock width [*Orlowski et al.*, 1995].

Turning to the simulations: When the shock is first forming, we find some transient, approximately group-standing whistlers that are generated by reflected or leaking ions. Soon after that, a phase-standing wave trains develops. Up to this point the results are similar to 1-D hybrid simulations (kinetic ions, fluid electrons) that we conducted for comparison, with the exception of strong electron Landau damping present here. However, at later times we find that eventually most of the phase-standing wavetrain is suppressed in favor of whistler waves that appear to propagate at some angle between **n** and $\mathbf{B_o}$. Figure 2 shows the compressional

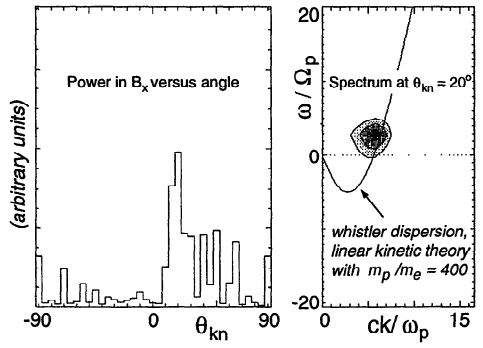

Figure 3. Spectral analysis of waves in Fig. 2*b*. Power peaks at $\theta_{kn} \sim 20°$; waves are on the whistler branch with upstream directed group and phase velocity.

field component B_y at (a) early times ($4\ {\Omega_p}^{-1}$) and (b) late times ($6\ {\Omega_p}^{-1}$) in the simulation, in the shock vicinity. The difference between the early, phase-standing waves and the later, oblique waves is quite evident. At both times the total shock width is approximately one ion inertial length, and it is a fraction of that (~ 0.25 to 0.5 c/ω_p or 5 to 10 c/ω_e) for the e-folding scale of the magnetic field. The latter is in fair agreement with the observations by *Scudder et al.* [1986].

Figure 3 shows a spectral diagnostic of the waves. There is finite power at all angles between **n** (0°) and -$\mathbf{B_o}$ (60°), with a peak propagation angle of $\theta_{kn} \sim 20°$ or $\theta_{kB} \sim 40°$, and upstream directed group and phase velocities. The frequency in the plasma rest frame is $\sim 30 \pm 5\ \Omega_p$, the wavelength 1 c/ω_p. Thus, we find that these waves have all the major properties of observed "one-Hertz waves" [*Orlowski et al.*, 1993, 1995]: they are finite bandwidth in the shock frame, generated in the ramp but propagate upstream, they are significantly Landau damped, and have **k** in the coplanarity plane at some small angle away from **n** but between **n** and $\mathbf{B_o}$, with $\theta_{kB} \sim 40°$.

An analysis of the proton phase space shows that the most likely free energy source for these waves is in the reflected, gyrating ions. While a detailed instability calculation remains to be carried out, it is known that the effective anisotropy contained in these ions can drive a variant of the cross-field streaming instability [*Wu et al.*, 1983]. This instability is not driven by the cross-field current. Rather, is related to the anisotropic proton beam instability advanced by *Wong and Goldstein* [1988] to explain upstream whistlers. The main difference here is that the waves are generated in the ramp by the gyrating ions that convect back into the shock, and not in situ upstream by a propagating ion beam as suggested by *Wong and Goldstein*. Indeed, these authors have shown that the growth rate maximizes at oblique propagation if the perpendicular energy of the ions is large, as in the present case.

Figure 4 shows y-averaged profiles of the total magnetic field and the parallel and perpendicular electron temperature (all normalized to upstream values). Also shown is the electron phase space $v_\perp \cdot f(v_\parallel, v_\perp)$, normalized with the upstream thermal velocity, at three selected regions: in the ramp, at the overshoot, and just downstream from the overshoot. There is a factor of two per contour line with an overlayed grey scale. Note that the averaging over y broadens the apparent shock profile. There is very little pre-shock heating of the electrons, although there is a finite upstream directed heat flux as evidenced by the ramp phase space. Although the averaging has diluted some of the finer details of the phase space, the tilt of the ramp distribution shows that it is the electrons with large magnetic moment μ that are preferentially reflected. There is a small temperature anisotropy $T_{e\perp}/T_{e\parallel} > 1$ in the vicinity of the overshoot. Note, however, that the maximum $T_{e\perp}$ is achieved just in front of the overshoot, and its value farther downstream is slightly below what is expected from μ-conservation. We interpret these findings as due to selective reflection of electrons with large μ. There may also be some cooling associated with the filling of the parallel phase space. Values of $T_{e\perp}$ slightly below expectations from μ-conservation have also been found in observations [*Scudder et al.*, 1986]. $T_{e\parallel}$ remains nearly constant downstream. The total energy gain ($E_{th_1} - E_{th_o} = 60$ eV -20 eV) is commensurate with the deHoffmann-Teller frame cross-shock potential determined from the simulation ($e\phi \sim 40$ eV). The distribution downstream from the overshoot has the characteristic shape that results in a flat-top when integrated over $v_\perp$.

Further analysis of the phase space will be presented in a separate publication. Here the central point is that the phase space evolution appears to be largely determined by the macroscopic fields, as originally conjectured by *Feldman et al.* [1983] and *Scudder* [1986] based on detailed spacecraft observations. It should be pointed out that the amount of scattering necessary is small here; it would be larger for a shock with a higher ratio of the cross-shock potential energy to the adiabatic perpendicular energy of the electrons. We find no evidence of additional heating, due to either electrostatic waves or due to strong non-adiabatic motion in a sharp gradient of $\phi(x)$, as was suggested by *Balikhin and Gedalin* [1994]. Note that while simulations with smaller mass ratio or fewer particles per cell may also result in flat-tops, such distributions can be due to a number of reasons, such as scattering in numerical (i.e., non-physical) waves, or unrealistic coupling of the proton and electron scales. The nearly adiabatic behavior of the electrons and lack of additional heating in the present simulations are from a physical viewpoint more significant features than the simple presence of a flat-top. The lack of signatures indicating strong free energy is also compatible with the idea that the upstream whistlers are generated by the reflected ions, with little kinetic contribution by the electrons. However, since these waves are strongly Landau damped, they may be

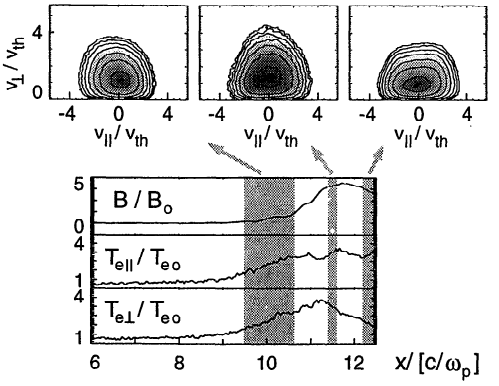

Figure 4. Electron phase-space, and cross-shock profiles of the magnetic field and parallel and perpendicular electron temperature, at the end of the simulation.

responsible for a slight pre-heating of the electrons in the vicinity of the ramp [c.f. *Liewer et al.*, 1991].

4. Summary

We presented the first 2-D full-particle simulations of a quasi-perpendicular shock with a large mass ratio $m_p/m_e = 400$. A large mass ratio is important to achieve the correct wave properties and particle thermalization at the shock. We find that a phase standing whistler wavetrain, which is not seen in satellite observations, is a transient feature. It is eventually replaced by upstream propagating oblique whistlers, most likely generated by the cross-field streaming instability of the reflected ions. The oblique waves satisfy all of the observed properties of upstream whistlers ("one-Hertz waves"). Given that phase-standing waves can only exist if the phase coherence of the ramp is not disturbed, the simulations can explain both the presence of the observed upstream whistlers and the absence of a phase-standing wavetrain. The electron phase-space evolution is largely adiabatic, in agreement with the observations by *Feldman et al.* [1983] and *Scudder* [1986]. The large mass ratio effectively decouples the kinetic evolution of the ions and the electrons.

Acknowledgments. The authors would like to thank K. B. Quest and D. S. Orlowski for many useful discussions. This work was supported by NASA's Space Physics Theory Program, research grant NAG5-1492, and NASA grant NAGW-2618. Work at Queen Mary and Westfield College was supported by PPARC grant GR/J36440. Computations were executed on Cray C-90s of the NSF San Diego Supercomputer Center and at the Atlas Centre, Rutherford Appleton Laboratory, UK.

References

Balikhin, M., and M. Gedalin, Kinematic mechanism of electron heating in shocks: Theory vs. observations, *Geophys. Res. Lett., 21,* 841–844, 1994.

Fairfield, D. H., Whistler waves observed upstream from collisionless shocks, *J. Geophys. Res., 79,* 1368–1378, 1974.

Feldman, W. C., R. C. Anderson, S. J. Bame, S. P. Gary, J. T. Gosling, D. J. McComas, M. F. Thomsen, G. Paschmann, and M. M. Hoppe, Electron velocity distributions near the Earth's bow shock, *J. Geophys. Res., 88,* 96–110, 1983.

Forslund, D. W., K. B. Quest, J. U. Brackbill, and K. Lee, Collisionless dissipation in quasi-perpendicular shocks, *J. Geophys. Res., 89,* 2142–2150, 1984.

Gurnett, D. A., Plasma waves and instabilities, in *Collisionless Shocks in the Heliosphere: Reviews of Current Research,* edited by B. T. Tsurutani and R. G. Stone, pp. 207–224, AGU, Washington, D. C., 1985.

Héron, A., and J. C. Adam, Particle code optimization on vector computers, *J. Comp. Phys., 85,* 284–301, 1989.

Hewett, D. W., and A. B. Langdon, Electromagnetic direct implicit plasma simulation, *J. Comp. Phys., 72,* 121–155, 1987.

Hoppe, M. M., and C. T. Russell, Plasma rest frame frequencies and polarizations of the low frequency upstream waves: ISEE1 and 2 observations, *J. Geophys. Res., 88,* 2021–2028, 1983.

Hoppe, M. M., C. T. Russell, L. A. Frank, T. E. Eastman, and E. W. Greenstadt, Characteristics of the ULF waves asociated with upstream ion beams, *J. Geophys. Res., 87,* 643–650, 1982.

Krauss-Varban, D., Simulation of electron acceleration at collisionless shocks, in *Particle Acceleration in Cosmic Plasmas,* edited by G. P. Zank and T. K. Gaisser, pp. 445–450, 1992.

Lembège, B., and J. M. Dawson, Plasma heating through a supercritical oblique collisionless shock, *Phys. Fluids, 30,* 1110–1114, 1987.

Leroy, M. M., D. Winske, C. C. Goodrich, C. S. Wu, and K. Papadopoulos, The structure of perpendicular bow shocks, *J. Geophys. Res., 87,* 5081–5094, 1982.

Liewer, P., V. K. Decyk, J. M. Dawson, and B. Lembège, Numerical studies of electron dynamics in oblique quasi-perpendicular collisionless shock waves, *J. Geophys. Res., 96,* 9455–9465, 1991.

McKean, M. E., N. Omidi, and D. Krauss-Varban, Wave and ion evolution downstream of quasi-perpendicular bow shocks, *J. Geophys. Res., 100,* 3427–3437, 1995.

Orlowski, D. S., and C. T. Russell, ULF waves upstream of the Venus bow shock: Properties of one-Hertz waves, *J. Geophys. Res., 96,* 11271–11282, 1991.

Orlowski, D. S., C. T. Russell, D. Krauss-Varban, and N. Omidi, On the source of upstream whistlers in the Venus foreshock, in *Plasma environments of non-magnetic planets,* edited by T. I. Gombosi, pp. 217–227, Pergamon Press, Oxford, 1993.

Orlowski, D. S., C. T. Russell, D. Krauss-Varban, N. Omidi, and M. F. Thomsen, Damping and spectral formation of broadband upstream whistlers, *J. Geophys. Res., 100,* in press, 1995.

Pantellini, F. G., A. Heron, J. C. Adam, and A. Mangeney, The role of the whistler precursor during the cyclic reformation of a quasi-parallel shock, *J. Geophys. Res., 97,* 1303–1311, 1992.

Savoini, P., and B. Lembège, Electron dynamics in two- and one-dimensional oblique supercritical collisionless magnetosonic shocks, *J. Geophys. Res., 99,* 6609–6635, 1994.

Sckopke, N., G. Paschmann, S. J. Bame, J. T. Gosling, and C. T. Russell, Evolution of ion distributions across the nearly perpendicular bow shock: Specularly and nonspecularly reflected gyrating ions, *J. Geophys. Res., 88,* 6121–6136, 1983.

Scudder, J. D., A. Mangeney, C. Lacombe, C. C. Harvey, and T. L. Aggson, The resolved layer of a collisionless high beta, supercritical quasi-perpendicular shock wave, 2, Dissipative fluid dynamics, *J. Geophys. Res., 91,* 11,053–11,073, 1986.

Tidman, D. A., and T. G. Northrop, Emission of plasma waves by the Earth's bow shock, *J. Geophys. Res., 73,* 1543–1553, 1968.

Veltri, P., and G. Zimbardo, Electron–whistler interaction at the Earth's bow shock, 2., Electron pitch angle diffusion, *J. Geophys. Res., 98,* 13,335–13,346, 1993.

Wong, H. K., and M. L. Goldstein, Proton beam generation of oblique whistler waves, *J. Geophys. Res., 93,* 4110–4114, 1988.

Wu, C. S., Y. M. Zhou, S. T. Tsai, S. C. Guo, D. Winske, and K. Papadopoulos, A kinetic cross-field streaming instability, *Phys. Fluids, 26,* 1259–1267, 1983.

D. Krauss-Varban, Department of Electrical and Computer Engineering, University of California, San Diego, 9500 Gilman Drive, La Jolla, California 92093-0407 (e-mail: varban@ece.ucsd.edu).

F. G. E. Pantellini, DESPA, Observatoire de Paris, Meudon, France.

D. Burgess, Astronomy Unit, Queen Mary and Westfield College, London, United Kingdom.

(received April 17, 1995; accepted May 29, 1995.)